

Relaxation of a two-dimensional electron gas in semiconductor thin films at low temperatures: Role of acoustic phonon confinement

B. A. Glavin and V. I. Pipa

*Department of Electrical and Computer Engineering, Wayne State University, Detroit, Michigan 48202
and Institute of Semiconductor Physics, Kiev, 03028, Ukraine*

V. V. Mitin

Department of Electrical and Computer Engineering, Wayne State University, Detroit, Michigan 48202

M. A. Stroschio

U.S. Army Research Office, P.O. Box 12211, Research Triangle Park, North Carolina 27709

(Received 11 September 2000; revised manuscript received 21 November 2001; published 13 May 2002)

We study the effect of acoustic-phonon confinement on the energy and momentum relaxation of a two-dimensional electron gas in thin films. The interaction via the deformation and piezoelectric potentials with a complete set of phonon modes in films with stress-free and rigid surfaces is taken into account. We demonstrate that in thin films the modification of the phonon properties and screening brings about substantial changes of the electron relaxation rates in comparison to the case of interaction with bulk phonons at low temperatures, where the effective reduction of the phonon spectrum dimensionality takes place. For suspended films, relaxation rates are substantially enhanced: the temperature dependence of the momentum and energy relaxation rates, in films with nonmetallized (metallized) surfaces, is found to be $T^{7/2}$ ($T^{5/2}$) for both deformation potential and piezoelectric mechanisms. The reason for such an enhancement is the strong scattering of electrons by flexural phonons having quadratic dispersion and a high density of states at low frequencies. Conversely, for films with rigid surfaces the low-temperature relaxation of electrons is exponentially suppressed due to the formation of a gap in the phonon spectrum.

DOI: 10.1103/PhysRevB.65.205315

PACS number(s): 73.50.Bk, 63.20.Dj, 72.15.Lh

I. INTRODUCTION

The problem of electron-phonon interaction in nanostructures has been studied for about 20 years. Basically, there are two principal phenomena that modify the process of electron scattering on the lattice vibrations in nanostructures. First, the reduction of the electron momentum space dimensionality brings about interesting properties of the electron-phonon interaction kinematics, controlled by the momentum and energy conservation laws.^{1,2} The second phenomenon arises due to the modifications of the phonon modes caused by the acoustic and dielectric mismatches of the materials forming the nanostructures. These changes in properties give rise to phonon minibands in superlattices, as well as to confined and interface phonons in quantum wells, quantum wires, and quantum dots. There is extended literature devoted to electron-phonon interactions in nanostructures embedded in bulk materials (see, e.g. the review in Refs. 3 and 4). In this paper we address the less investigated problem of the two-dimensional electron gas (2DEG) interaction with confined, resonatorlike acoustic phonons in thin films. The complete confinement of acoustic modes between the surfaces of a structure can be ideally achieved in structures that are spatially separated from the substrate for most of their extent (so-called *free-standing* or *suspended* structures). Free-standing quantum nanostructures made of various semiconductors and metals fabricated of different shape and sizes provide two-, one-, or zero-dimensional confinement of electrons and acoustic phonons (see, e.g., the review in Ref. 5). Such nanostructures have attracted interest because of their

potential applications, and their importance in understanding the physics of low-dimensional systems. The quantization of the acoustic-phonon spectrum in such structures manifests itself in optical,⁶ electrical,⁷ and recent heat-transport⁸ measurements. The effect of extreme confinement of acoustic phonons on Peierls transition⁹ and on electron-phonon scattering¹⁰⁻¹² in free-standing quantum wires has been investigated theoretically. Previous results¹⁰⁻¹² demonstrated the profound effect of different mechanical boundary conditions on electron-phonon scattering rates. In experiments¹³ and theory¹⁴ the temporal behavior of the lowest-order non-equilibrium spheroidal acoustic mode in spherical quantum dots of PbS was investigated. Recently, suspended nanostructures received much attention as mesoscopic mechanical systems having the quantum behavior in the conductance of heat by phonons.¹⁵⁻¹⁹

In nanoscale films, the acoustic-phonon spectrum is represented by the series of branches $\omega(\mathbf{q})$, where \mathbf{q} is a two-dimensional (2D) phonon wavevector. At high temperatures, electrons can interact with a huge number of phonon modes. Commonly, this cancels effect of the phonon confinement, and the electron relaxation characteristics are the same as in bulk crystals. However, if the temperature falls below the characteristic phonon mode spacing, only the lowest phonon branches contribute to electron scattering. In this case, an effective reduction of the phonon dimensionality takes place which affects essentially electron scattering. Previously, several authors claimed that a reduction of the phonon dimensionality should modify the temperature dependence of the electron relaxation characteristics causing their enhancement

(see, for example, Ref. 20). For semiconductors, this effect was observed in Ref. 21 for 2D holes confined in a Ge/SiGe heterostructure. In this paper we examine the impact of acoustic phonon confinement in isolated films. We demonstrate that a reduction of the phonon dimensionality is not the only reason modifying the electron relaxation. In addition to the reduced dimensionality, low-frequency phonons in thin films possess unique properties strongly dependent on the mechanical properties at the surfaces. So, for free-standing films, flexural phonons exist that have quadratic dispersion. We show that flexural phonons cause effective electron scattering. This is due to the high density of states of such phonons. As a result, the momentum and energy relaxation rates in free-standing films are substantially enhanced compared to the case of scattering in bulk crystals, and obey a $T^{7/2}$ temperature dependence provided that screening is taken into account. It is important that this temperature dependence holds both for deformation potential (DP) and piezoelectric (PA) mechanisms of electron-phonon interaction. In the opposite case of rigid-surface films, a gap appears in the low-frequency region of the phonon spectrum. Consequently, the electron relaxation rates are suppressed exponentially at low temperatures. Note that a similar effect was detected for quantum dots, where gaps in the phonon spectrum exist due to its the purely discrete character.^{22,23}

Similar problems were addressed previously in Refs. 5, 24 and 25 by means of numerical calculations for the case of unscreened DP electron-phonon interaction. In Refs. 5 and 24 the choice of a particular system, a free-standing quantum well where the regions of the electron and phonon confinement coincide, canceled the interaction of electrons with flexural phonons due to the symmetry properties of the system. In Ref. 25 a more general case of a quantum well situated inside a wider film was analyzed briefly. In the present paper we obtain asymptotic dependences of the relaxation rates in free-standing and rigid-surface films at low temperatures for both DP and PA electron-phonon interactions, and present the results of corresponding numerical calculations. As in Ref. 25, we assume an asymmetric placement of the quantum well inside the film, which allows electron coupling with flexural phonons. We also analyze the peculiarities of screening of the electron-phonon interaction in films, and discuss the role of the electrical conditions at the film surfaces.

The paper is organized as follows. In Sec. II we describe the peculiarities of the acoustic-phonon modes in a film with stress-free and rigid surfaces. In Sec. III, general expressions for the matrix elements of the electron-phonon interaction via the deformation and piezoelectric potentials and the equation for momentum and energy relaxation rates are derived. Then, in Sec. IV, we obtain the low-temperature asymptotes of the electron relaxation rates. The results of the numerical calculations are presented and discussed in Sec. V. Finally, in Sec. VI, we present the principal conclusions of this work. The phonon modes, screening factor in films, and the role of the nonequilibrium phonon buildup in free-standing films are described in the Appendixes.

II. ACOUSTIC PHONON CONFINEMENT IN FILMS

We consider an infinite film of the width a , and take the z axis to be perpendicular to the film surface, the plane $z=0$ corresponds to middle plane of the film. The electron confinement is due to the double heterostructure quantum well having, in general, a different width and asymmetric placement inside the film. For simplicity, we assume that the elastic properties of the film are isotropic and characterized by the same constants in the quantum well and the barrier regions. These assumptions make it possible to consider the main qualitative peculiarities of the electron-phonon interaction brought about by the phonon confinement, and, on the other hand, to express the results without very complex formulas. Assuming that the film is uniform, we do not produce a large error because typically the elastic properties of the materials forming the nanostructure do not differ a lot. For example, for a GaAs/AlAs heterostructure the mismatch of the density is about 25%, and the mismatch of the elastic constants is about a few percent.

In the isotropic elastic continuum approximation, the lattice displacement \mathbf{u} obeys the equation

$$\frac{\partial^2 \mathbf{u}}{\partial t^2} = s_l^2 \nabla^2 \mathbf{u} + (s_l^2 - s_t^2) \nabla (\nabla \cdot \mathbf{u}), \quad (1)$$

where s_l and s_t are the velocities of longitudinal and transverse bulk acoustic waves. The confined phonons are plane waves $\mathbf{u} = \mathbf{u}_0(z) \exp[i(\mathbf{q}\mathbf{r} - \omega t)]$, where $\mathbf{q} = (q_x, q_y)$ is the in-plane wave vector and $\mathbf{r} = (x, y)$. We will use the following notations: $u_0^{(z)}$ is the z component of \mathbf{u}_0 , and $u_0^{(\parallel)}$ and $u_0^{(\perp)}$ are the in-plane components parallel and perpendicular to \mathbf{q} , respectively.

To define a system of the confined modes, Eq. (1) should be complemented by the boundary conditions at the film surfaces $z = \pm a/2$. We will concentrate on the following two limiting cases: a film with stress-free boundaries and a film with rigid boundaries. In the first case, the boundary conditions are imposed on the stress tensor: $\sigma_{zx} = \sigma_{zy} = \sigma_{zz} = 0$ at $z = \pm a/2$. They reflect the fact that there is not any force acting on the film surfaces from the surrounding media. For a film with rigid surfaces, the boundary conditions are $\mathbf{u}_0(z = \pm a/2) = 0$. Since both these types of boundary conditions do not depend on the elastic parameters of a surrounding medium, the phonon subsystem in such films can be considered as isolated.

The procedure of obtaining the eigenphonon modes is straightforward. For suspended films, it was described in Ref. 26. We briefly present the dispersion equation as well as eigendisplacements for both suspended and rigid-surface films in Appendix A. Here we would like to summarize the qualitative properties of the acoustic phonon modes.

There are three types of modes, that differ by the kind and the symmetry of displacement components. For the first of them, the dilatational modes $u_0^{(z)}$ is an odd function of z , while $u_0^{(\parallel)}$ is an even function of z (with respect to the mid-plane). For the modes of the second type, the flexural modes $u_0^{(z)}$ is even and $u_0^{(\parallel)}$ is an odd function of z . For both of these modes $u_0^{(\perp)} = 0$. Finally, the third type of modes the horizon-

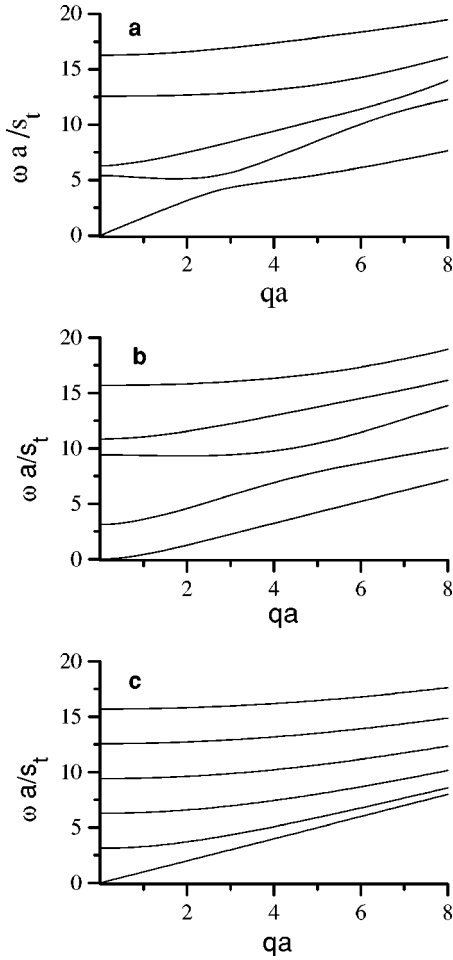


FIG. 1. Acoustic phonon spectrum for a film with stress-free boundaries: dilatational modes (a), flexural modes (b), and horizontal shear modes (c).

tal shear modes, have only a nonzero displacement $u_0^{(\perp)}$ which is perpendicular to the direction of wave propagation and lies in the plane of film; $u_0^{(\perp)}(z)$ is either an odd or even function of z . In Figs. 1 and 2 we show the dispersion curves of few lower phonon modes for suspended and rigid-surface films, respectively. In calculations we assumed $s_t = 3.02 \times 10^5$ cm/s and $s_l = 5.22 \times 10^5$ cm/s.

In the following, the low-frequency phonon modes will be especially important to us, since such phonons play a key role in the processes of the electron scattering at low temperatures. One can see from Figs. 1 and 2 that the phonon properties in this range differ drastically for the two types of mechanical conditions at the surface. For a free-surface film, there are three “acoustic” branches with $\omega \rightarrow 0$ at $q \rightarrow 0$. Two of them, dilatational modes and horizontal shear modes, have a linear dispersion at small q , $\omega \sim q$, while the flexural modes have a quadratic dispersion $\omega \sim q^2$. Accordingly, the flexural modes have a high density of states at small q , which, as we will see below, gives rise to an enhancement of the electron scattering.

Conversely, in a film with the rigid surfaces there are no “acoustic” modes. The phonon spectrum at $q \rightarrow 0$ has a gap $\Delta\omega \sim \pi s_t/a$. Therefore, there should be a strong suppression

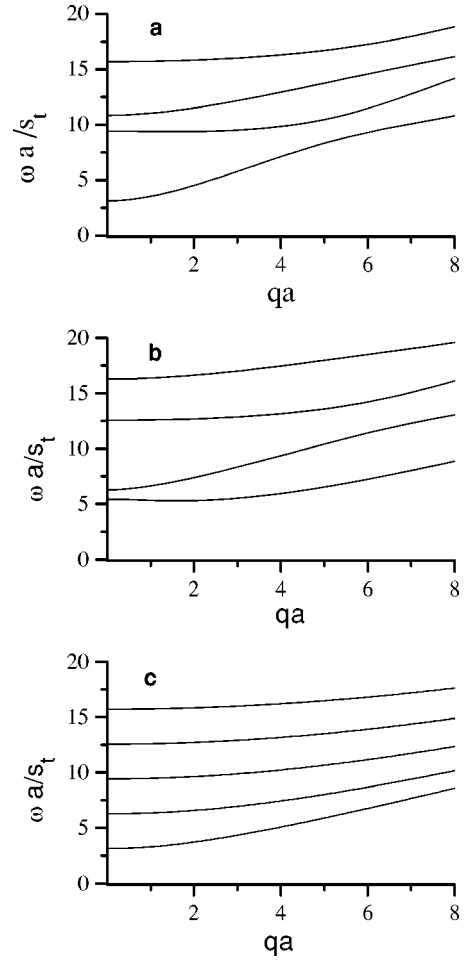


FIG. 2. Acoustic phonon spectrum for a film with rigid boundaries: dilatational modes (a), flexural modes (b), and horizontal shear modes (c). The spectra of all three types of modes have gaps in the low-frequency region.

of the electron-phonon interaction at low temperatures, since electrons have no phonons to interact with. It is important to note that the gap in the phonon spectrum is conserved even for a film with only one rigid surface. For example, for a film with one free surface and one rigid surface we obtained a value of the gap which is half that of a film with two rigid surfaces.

III. EQUATIONS FOR THE RELAXATION RATES OF 2D ELECTRONS

In this paper, we calculate such characteristics of the electron-phonon interaction as electron momentum and energy relaxation rates due to scattering with equilibrium confined acoustic phonons with lattice temperature T . Electrons will be assumed to be concentrated on the lowest subband of a quantum well with a wave function $\chi(z)\exp(i\mathbf{k}\mathbf{r})/\sqrt{S}$, where S is the normalizing area. Momentum and energy relaxation rates $1/\tau_m$ and $1/\tau_e$, respectively, are defined as parameters characterizing a transfer of the average momentum per electron and energy per electron to the crystal lattice due to intrasubband scattering. We use the model electron distri-

bution function for the case of a weak electric field:

$$f = \left[1 + \exp\left(\frac{\varepsilon_k - \hbar \mathbf{k} \mathbf{v}_{dr} - \varepsilon_F}{T_e}\right) \right]^{-1}. \quad (2)$$

Here $\varepsilon_k = \hbar^2 k^2 / 2m$ is the electron energy, m is effective mass, ε_F is the Fermi energy, \mathbf{v}_{dr} is the drift velocity, and T_e is the electron temperature differing from the lattice temperature T (the temperature is measured in energy units). The shifted Fermi-Dirac distribution function of Eq. (2) is well justified for the case of strong electron-electron scattering. The time scale for electron-electron scattering is estimated as $\tau_{e-e} \approx (\hbar / \varepsilon_F) (\varepsilon_F / T)^2$ (see Ref. 27). For a 2DEG in GaAs with an electron concentration $n = 10^{11} \text{ cm}^{-2}$ and $T \sim 1 \text{ K}$, $\tau_{e-e} \sim 10^{-10} \text{ s}$. This value is small compared to the relaxation times obtained in our calculations: see Figs. 3–6.

For weakly nonequilibrium electrons, the momentum relaxation rate relates the weak electric field F and the drift velocity \mathbf{v}_{dr} , while the energy relaxation rate relates small temperature difference $T_e - T$ and the rate of electron energy losses per unit area, W ,

$$\mathbf{v}_{dr} = \frac{e \tau_m}{m} F, \quad (T_e - T)n = W \tau_e, \quad (3)$$

where n is the electron density. Note that in contrast to the momentum relaxation rate, the energy relaxation rate, being determined by the scattering with phonons, conserves its rigorous meaning in the presence of intensive elastic scattering on defects. Using the distribution function of Eq. (2), in the case of small deviation from thermodynamic equilibrium, we obtain

$$\frac{1}{\tau_m} = \frac{\hbar^2}{nmST} \sum_{\mathbf{k}, \mathbf{k}'} (k \cos \varphi - k' \cos \varphi')^2 W_{\mathbf{k}, \mathbf{k}'} \times [1 - f_0(k')] f_0(k), \quad (4)$$

$$\frac{1}{\tau_e} = \frac{1}{nST^2} \sum_{\mathbf{k}, \mathbf{k}'} (\varepsilon_k - \varepsilon_{k'})^2 W_{\mathbf{k}, \mathbf{k}'} [1 - f_0(k')] f_0(k). \quad (5)$$

Here f_0 is the equilibrium distribution function, corresponding to Eq. (2) with $\mathbf{v}_{dr} = 0$ and $T_e = T$; $W_{\mathbf{k}, \mathbf{k}'}$ is the probability of the electron transitions $\mathbf{k} \rightarrow \mathbf{k}'$, S is the normalizing area, and φ is the polar angle between the electric field and the electron wave vector \mathbf{k} . The probability $W_{\mathbf{k}, \mathbf{k}'}$ is defined as

$$W_{\mathbf{k}, \mathbf{k}'} = \frac{2\pi}{\hbar} \sum_{\lambda} | \langle i | \hat{H}_{\lambda} | f \rangle |^2 | \epsilon |^{-2} \delta(E_i - E_f), \quad (6)$$

where \hat{H}_{λ} is the Hamiltonian of the electron-phonon interaction; λ labels the phonon modes; i, f and E_i, E_f denote the initial and final states and the energies of the electron-phonon system in these states; and ϵ is the screening factor of the 2D electrons derived in Appendix B. We take into account the DP and PA mechanisms of the electron-phonon interaction. For one mode (we drop for brevity a mode's label)

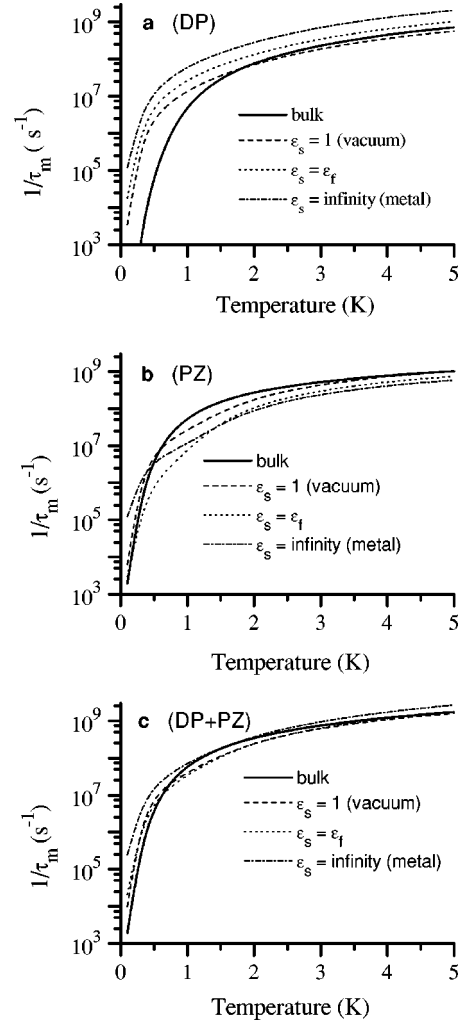


FIG. 3. Momentum relaxation rates vs temperature of a 2DEG in a film with stress-free surfaces. The dielectric permittivity of a material surrounding the film, ε_s , is different from the lattice dielectric permittivity of the film, ε_f . The relaxation rates due to interaction with confined phonons via the deformation potential, piezoelectric mechanism, and the total rates are presented in plots (a), (b) and (c), respectively; the cases $\varepsilon_s = 1$, ε_f , and ∞ correspond to the dashed, dotted, and dot-and-dashed curves. The solid curves correspond to relaxation rates of the 2DEG due to scattering on bulk phonons in unbounded medium.

$$\hat{H} = \sqrt{\frac{\hbar}{2\rho\omega S}} [V_{DP}(z) + e\phi_{PA}(z)] (\exp(i\mathbf{q}\mathbf{r}) \hat{b}_{\mathbf{q}} + \text{H.c.}), \quad (7)$$

$$V_{DP} \equiv E_1 \left(iqu_0^{(\parallel)} + \frac{du_0^{(z)}}{dz} \right),$$

where E_1 is the deformation potential constant, $\phi_{PA}(z)$ is the macroscopic electric potential induced by the deformation of the piezoelectric crystal, and $\hat{b}_{\mathbf{q}}$ is the phonon annihilation operator. The simultaneous action of the two mechanisms of the electron-phonon interaction in general gives rise to the interference between them, so

$$| \langle i | \hat{H}_{DP} + \hat{H}_{PA} | f \rangle |^2 \neq | \langle i | \hat{H}_{DP} | f \rangle |^2 + | \langle i | \hat{H}_{PA} | f \rangle |^2.$$

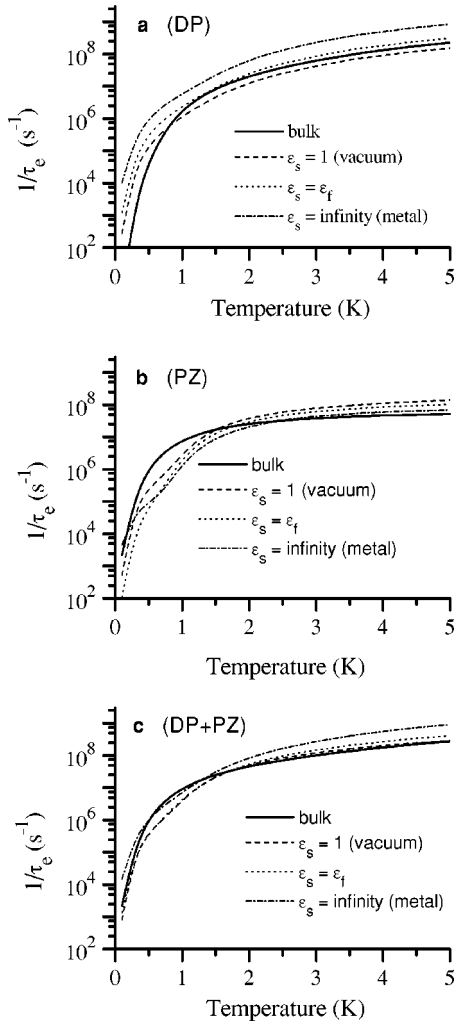


FIG. 4. Energy relaxation rates of a 2DEG in a film with stress-free surfaces; the conditions and notations are the same as in Fig. 3.

In the case of interaction with bulk phonons, perturbations induced by DP and PA couplings have a relative phase of $\pi/2$, and interference vanishes. However, this is not the case for the confined modes. Qualitatively, this can be explained in the following way. Confined modes are formed due to the interference between elastic waves, that are reflected multiple times from the film surfaces. Reflection causes mutual transformations of the longitudinal and transverse waves as well as phase shifts of these constituting waves. As a result, the interference between the DP and PA interactions does not vanish (with the exception of the shear modes, which are purely transverse waves and therefore do not interact with an electron via the deformation potential). Note that a similar interference effect was discussed previously for electron scattering on the acoustic waves of semi-infinite media.^{28,29} It is worth mentioning that in films interference can be especially important. As we demonstrate below, relaxation rates due to DP and PA scatterings in films have the same temperature dependence, which is different from the case of scattering in bulk crystals. Therefore, the interference term can be important in a wide range of temperatures.

In the present paper, we will deal with the case when the

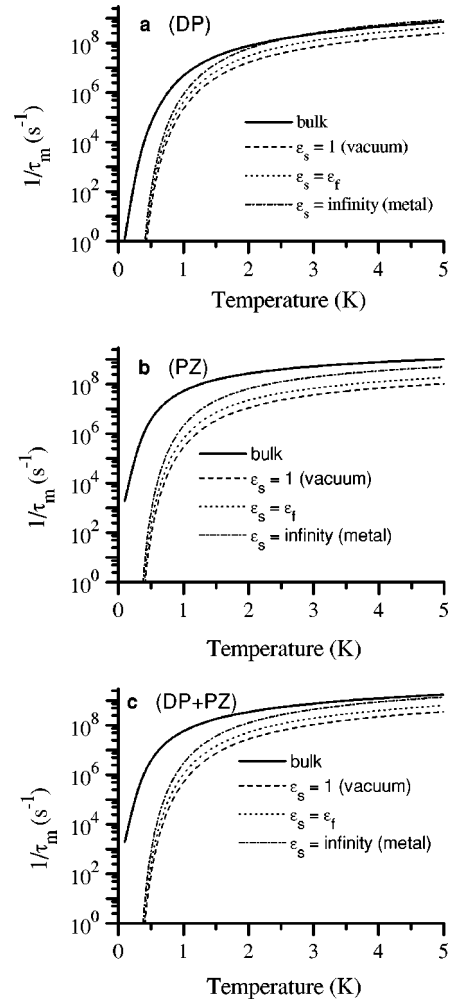


FIG. 5. Momentum relaxation rates of a 2DEG in a film with rigid surfaces; the conditions and notations are the same as in Fig. 3.

film is made from a material of cubic symmetry and its surface is parallel to the (100) crystal plane. As we will show below, for such a case the contributions of interference terms to the relaxation rates are canceled upon averaging over the final electron states.

For the piezoelectric potential we have an equation

$$\frac{d^2 \phi_{PA}}{dz^2} - q^2 \phi_{PA} = \frac{2e_{14}}{\epsilon_f \epsilon_0} \left(iq_x \frac{du_0^{(y)}}{dz} + iq_y \frac{du_0^{(x)}}{dz} - q_x q_y u_0^{(z)} \right), \quad (8)$$

where e_{14} is the only piezoelectric constant of a cubic crystal, ϵ_f and ϵ_0 are the relative permittivity of the film and the absolute dielectric constant, and the x and y axes coincide with the crystal axes of the fourth order. The boundary conditions for ϕ_{PA} are

$$\phi_{PA}|_{\pm a/2} = \phi_{PA}^s|_{\pm a/2},$$

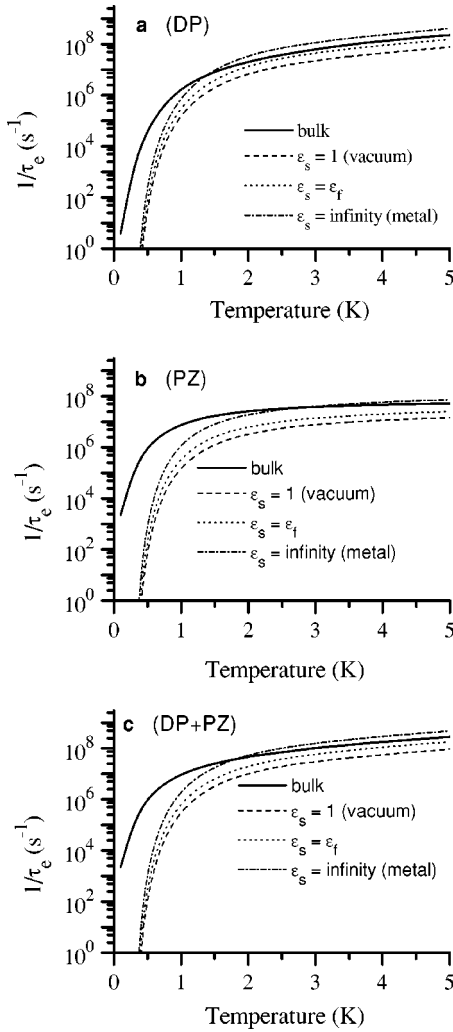


FIG. 6. Energy relaxation rates of a 2DEG in a film with rigid surfaces; the conditions and notations are the same as in Fig. 3.

$$\left(\epsilon_f \frac{d\phi_{PA}}{dz} - \frac{ie_{14}}{\epsilon_0} (q_x u_0^{(y)} + q_y u_0^{(x)}) \right) \Big|_{\pm a/2} = \epsilon_s \frac{d\phi_{PA}^s}{dz} \Big|_{\pm a/2}, \quad (9)$$

where ϕ_{PA}^s is the potential in the medium surrounding the film, ϵ_s is the dielectric permittivity of this medium. ϕ_{PA}^s satisfies Eq. (8) with $e_{14}=0$ and obeys zero boundary conditions at $z=\pm\infty$. Note that in the limit of $\epsilon_s \rightarrow \infty$, the boundary conditions of Eq. (9) are reduced to the conditions $\phi_{PA}(z=\pm a/2)=0$, corresponding to the case of metallized surfaces.

As we showed in Sec. II, phonon modes have either components $u_0^{(\parallel)}$, $u_0^{(z)}$ (dilatational and flexural modes), or $u_0^{(\perp)}$ (shear modes). If we introduce an angle φ_q between the phonon wave vector \mathbf{q} and the x axis, then $\phi_{PA}(z, \mathbf{q})$ can be written as $\phi_{PA} = \tilde{\phi}_{PA}(z, q)g(\varphi_q)$, where

$$g(\varphi_q) = \begin{cases} \sin \varphi_q \cos \varphi_q \\ \cos^2 \varphi_q - \sin^2 \varphi_q \end{cases}. \quad (10)$$

Here, the upper line corresponds to the dilatational or flexural modes, while the lower line corresponds to the shear modes.

In order to calculate the momentum relaxation rate, in Eq. (4) we change the integration over electron wave vectors k and k' , the angle φ' to the integration over the electron energies ε and ε' , and the angle ψ between \mathbf{k} and \mathbf{k}' to $\psi = \varphi - \varphi'$. We obtain

$$\begin{aligned} \frac{1}{\tau_m} = & \frac{m^2}{8\pi\hbar^4\rho nT} \sum_{j,\eta} \int d\varepsilon d\varepsilon' d\varphi d\psi f_0(\varepsilon)(1-f_0(\varepsilon')) \\ & \times |\Phi_{DP} + g\Phi_{PA}|^2 (\sqrt{\varepsilon} \cos \varphi - \sqrt{\varepsilon'} \cos(\psi - \varphi))^2 \\ & \times \delta(\varepsilon - \varepsilon' + \eta\hbar\omega) \frac{1}{\omega|\varepsilon|^2} \left(N_\omega + \frac{1-\eta}{2} \right). \end{aligned} \quad (11)$$

Here and hereafter, we use the common label j to denote the acoustic branches of all types of modes; $\eta=1$ corresponds to phonon absorption and $\eta=-1$ to phonon emission. The magnitudes q and φ_q are determined by the momentum conservation $\mathbf{k}' = \mathbf{k} + \eta\mathbf{q}$, $N_\omega = (\exp(\hbar\omega/T) - 1)^{-1}$ is the Planck distribution function for phonons, and

$$\Phi_{DP} = \int dz \chi^2(z) V_{DP}, \quad \Phi_{PA} = e \int dz \chi^2(z) \tilde{\phi}_{PA}. \quad (12)$$

In Eq. (11), the integration over the angle φ is carried out straightforwardly, and cancels the linear terms in g which are responsible for interference of the DP and PA mechanisms. This results in independent contributions of these mechanisms to the relaxation rate.

For further calculations, it is convenient to change the integration over the angle ψ to an integration over the wave vector q using the momentum conservation law, giving

$$q^2 = \frac{2m}{\hbar^2} (\varepsilon + \varepsilon' - 2\sqrt{\varepsilon\varepsilon'} \cos \psi). \quad (13)$$

Upon integration over ε' , Eq. (11) can be finally rewritten as

$$\begin{aligned} \frac{1}{\tau_m} = & \frac{1}{16\pi^2\rho nT} \sum_{j,\eta} \int d\varepsilon dq \frac{q^3 f_0(\varepsilon)}{\omega\sqrt{\varepsilon}} \\ & \times \frac{1-f_0(\varepsilon + \eta\hbar\omega)}{\sqrt{\varepsilon + \eta\hbar\omega} |\sin \psi_\eta|} |\varepsilon|^2 \left(N_\omega + \frac{1-\eta}{2} \right) |M_j|^2. \end{aligned} \quad (14)$$

Here $|M_j|^2 = |\Phi_{DP}^j|^2 + \alpha_j |\Phi_{PA}^j|^2$ and α_j is a constant, resulting from the integration of the squared matrix element of the PA interaction over φ ; for the dilatational and flexural modes $\alpha_j = 1/8$ and for the horizontal shear modes $\alpha_j = 1/2$. It is worth mentioning that the same numerical coefficients α_j appear in an isotropic model where the squared matrix elements of PA interaction, initially averaged over azimuthal angle, are used. The angles ψ_η are the values of ψ allowed by the energy and momentum conservation laws. Analogously, Eq. (5) for the energy relaxation rate reduces to

$$\frac{1}{\tau_e} = \frac{m}{8\pi^2 \rho n T^2} \sum_{j,\eta} \int d\epsilon dq \frac{q \omega f_0(\epsilon)}{\sqrt{\epsilon(\epsilon + \eta \hbar \omega)}} \times \frac{[1 - f_0(\epsilon + \eta \hbar \omega)]}{|\sin \psi_\eta| |\epsilon|^2} \left(N_\omega + \frac{1-\eta}{2} \right) |M_j|^2. \quad (15)$$

Equations (14) and (15) are used in the present paper for numerical calculations of the momentum and energy relaxation rates. To study the peculiarities which stem from confinement nature of acoustic phonons, we will also calculate the relaxation rates in a 2D electron channel placed in the boundless semiconductor. To obtain these bulk relaxation rates, we calculate the rates given by Eqs. (14) and (15) in a thick film. The sought-for values, which correspond to the electron scattering on conventional bulk phonons, are found when the calculated rates do not depend on the film thickness.

We do not provide the general formulas for Φ_{DP} and Φ_{PA} , that are used in numerical calculations, due to their complexity. In Sec. IV we will present the small-frequency asymptotes relevant for electron relaxation at low temperatures.

IV. RELAXATION RATES AT LOW TEMPERATURES

In this section we obtain analytical expressions for relaxation rates at low temperatures, where the confinement nature of the phonon modes is most pronounced. By ‘‘low’’ temperatures, we mean the region when the interaction with the lowest branches of the phonon spectrum gives the dominant contribution to the relaxation rates. We introduce a characteristic temperature

$$T_f = \frac{\hbar s_t}{a}, \quad (16)$$

through which the mentioned condition can be rewritten as $T \ll T_f$. For real materials, T_f is small. For example, for $a = 10$ nm and $s_t = 3000$ m/s, T_f corresponds to 2 K. Consistent with the condition $T \ll T_f$, for typical semiconductor materials, the two following assumptions can be made. First, electrons can be treated as strongly degenerate even for moderate electron concentrations. Second, we assume that the Bloch-Grüneisen regime of low-angle electron scattering is realized; it can be shown that the characteristic temperature of the transition to the Bloch-Grüneisen regime is about T_f for $k_F \sim 1/a$, k_F being the Fermi wave vector.

For degenerate electrons, Eqs. (14) and (15) are substantially simplified. Due to the small deviation of electron energies from the Fermi energy ϵ_F , one can replace the energy ϵ by ϵ_F and neglect the energy transfer $\hbar \omega$ everywhere in Eqs. (14) and (15) except for the rapidly varying functions $f_0(\epsilon)$ and $f_0(\epsilon \pm \hbar \omega)$. As a result, Eq. (13) is simplified to the commonly used relation $q = 2k_F \sin(\psi/2)$. Using the remarkable relationship between the Fermi and Planck distribution functions,

$$\int_0^\infty d\epsilon f_0(\epsilon) [1 - f_0(\epsilon - \hbar \omega)] = N(\omega) \hbar \omega \quad (17)$$

and assuming small-angle scattering, we can express the relaxation rates in the following form:

$$\left\{ \begin{array}{l} 1/\tau_m \\ 1/\tau_e \end{array} \right\} = \frac{\sqrt{2m\hbar^2}}{16\pi\rho\epsilon_F^{3/2}T^2} \sum_j \int_0^\infty \frac{dq |M_j|^2}{|\epsilon|^2 \sinh^2(\hbar\omega_j/2T)} \left\{ \begin{array}{l} Tq^2/2m \\ \omega_j^2 \end{array} \right\}. \quad (18)$$

Here the summation over j can be restricted by the lowest branches of the flexural, dilatational, and shear modes, and we can use low- q expansions of M_j and ϵ .

First let us analyze the temperature dependence of the relaxation rates in a film with stress-free nonmetallic surfaces. In this case, $\epsilon(q)$ is given by Eq. (B6) and varies as q^{-1} . From the dispersion equations given in Appendix A in the small- q limit, one can obtain

$$\omega_f = s_t a \xi q^2, \quad \omega_d = 2\sqrt{3}\xi s_t q, \quad \omega_s = s_t q, \quad (19)$$

where $\xi = \sqrt{(1 - s_t^2/s_l^2)/3}$. For DP coupling, using expressions for the eigendisplacements provided in Appendix A, for flexural (f) and dilatational (d) modes: we obtain

$$V_{DP}^{(f)} = -\frac{2iE_1 s_t^2 q^2}{s_l^2 \sqrt{a}} z, \quad V_{DP}^{(d)} = \frac{2E_1 s_t^2 q}{s_l^2 \sqrt{a}}. \quad (20)$$

For shear modes, $V_{DP}^{(s)} = 0$. Substitution of these expressions into Eq. (18) shows that the contribution of flexural phonons to $1/\tau_m$ and $1/\tau_e$ is proportional to $T^{7/2}$, while the contribution of the dilatational phonons is proportional to T^6 for momentum relaxation and to T^5 for energy relaxation. Thus, at low temperatures, flexural phonons provide the dominant contribution to the relaxation rates. Neglecting by contribution of dilatational phonons, finally we have

$$\frac{1}{\tau_m} = \frac{105}{128} \frac{\zeta(7/2)}{\sqrt{2\pi}\xi^{9/2}} E_1^2 \frac{a_B^2 \mu_1^2}{m^{1/2} \rho a^{7/2} s_l^4 s_t^{1/2} \epsilon_F^{3/2} \hbar^{5/2}} \left(\frac{\epsilon_s}{\epsilon_f} \right)^2 T^{7/2}, \quad (21)$$

where ζ is the Riemann ζ function,³⁰ a_B is the effective Bohr radius, and μ_1 is an integral:

$$\mu_1 = \frac{1}{a} \int z \chi^2(z) dz. \quad (22)$$

The $T^{7/2}$ power law is valid when $\mu_1 \neq 0$, i.e., in the case of asymmetric distribution of the 2D electron density in respect to the midplane of film.

The long-wavelength asymptotes of the piezoelectric potentials induced by the lowest modes are given by

$$\begin{aligned} \bar{\phi}_{PA}^{(f)} &= P \frac{q^2}{\sqrt{a}} \left(\frac{a^2}{4} - z^2 \right), \\ \bar{\phi}_{PA}^{(d)} &= P \frac{qz}{\sqrt{a}}, \quad \bar{\phi}_{PA}^{(s)} = iP \frac{qz}{2\sqrt{a}}, \end{aligned} \quad (23)$$

where $P = ee_{14}/(\epsilon_f \epsilon_0)$ and the subscripts mark the type of the phonon mode. It is easy to verify that dilatational and shear modes give rise to dependencies $\tau_m^{-1} \sim T^6$ and τ_e^{-1}

$\sim T^5$. The main contribution to the relaxation rates proportional to $T^{7/2}$ again comes from the flexural modes, and we obtain

$$\frac{1}{\tau_m} = \frac{105}{16^4} P^2 \left(\frac{\epsilon_s}{\epsilon_f} \right)^2 \frac{\zeta(7/2)}{\sqrt{2\pi\xi^{9/2}}} \frac{a_B^2 \mu_2^2}{\rho \epsilon_F^{3/2} \hbar^{5/2} s_l^{9/2} a^{3/2} m^{1/2}} T^{7/2}. \quad (24)$$

Here μ_2 is determined according to the equation

$$\mu_2 = 1 - \int \frac{4z^2}{a^2} \chi^2(z) dz. \quad (25)$$

The energy relaxation rates associated with DP and PA scatterings are expressed through the corresponding momentum relaxation rates as

$$\frac{1}{\tau_e} = \frac{9\zeta(9/2)ma\xi s_l}{\zeta(7/2)\hbar} \frac{1}{\tau_m}. \quad (26)$$

According to these results, the momentum and energy relaxation rates have the same temperature dependence $T^{7/2}$ for both considered mechanisms of interaction, in contrast to the case of interaction of a 2DEG with bulk phonons, where $1/\tau_m \sim T^7$, $1/\tau_e \sim T^6$ for the DP interaction and $1/\tau_m \sim T^5$, $1/\tau_e \sim T^4$ for the PA interaction.³¹ The resulting weaker temperature dependencies show that, at low temperatures, electron relaxation on confined acoustic phonons is enhanced in comparison with the relaxation via scattering on bulk phonons.

In actual films, electron-phonon interaction can be modified due to the presence of close metal electrodes. In this paper we attempt to model their influence by considering the electron relaxation in films with metallized surfaces. This case demands special consideration. Calculating the relaxation rates due to phonons in a slab covered by metal film, we will neglect their change caused by Coulomb coupling between electrons in the QW and electrons in the metal film. Measurements³² of the coupling between 2D and 3D electron gases showed that the drag was small. According to Ref. 33, due to screening in the passive layer, the influence of this layer on the mobility in a 2DEG decreases as the temperature decreases and/or the concentration of carriers in the passive layer increases. In the case of low temperatures (~ 1 K), which is interesting for us the change of relaxation due to interlayer electron-electron collisions can be neglected.

From Eq. (B7) it follows that in metallized film, screening of the electron-phonon interaction is suppressed: in the long-wavelength limit, $\epsilon(q)$ does not depend on q . The DP interaction is altered in the presence of metal only by the change in screening. As a result, the previously obtained power law $T^{7/2}$ is reduced to a $T^{5/2}$ power law

$$\frac{1}{\tau_m} = \frac{15}{16} \frac{\zeta(5/2)}{\sqrt{2\pi\xi^{7/2}}} E_1^2 \frac{\mu_1^2 s_l^{1/2}}{m^{1/2} \rho a^{5/2} s_l^4 \epsilon_F^{3/2} \hbar^{3/2} \epsilon_m^2} T^{5/2}, \quad (27)$$

where the screening factor, $\epsilon_m = \epsilon(q \rightarrow 0)$, is given by Eq. (B7).

The PA scattering experiences a dual influence as a result of the surface metallization. The metal-induced modification of the PA interaction originates not only from the reduction of the screening but also from a modification of the bare piezoelectric potential, and is also due to the vanishing of the potential at a metal surface. The PA potential associated with the lowest flexural mode conserves the dominant role in electron scattering, and results in

$$\frac{1}{\tau_m} = \frac{15\sqrt{2}\zeta(5/2)}{\sqrt{\pi}4^9} \frac{P^2 \mu_2^2}{\rho \epsilon_F^{3/2} \hbar^{3/2} (s_l \xi)^{7/2} a^{1/2} m^{1/2} \epsilon_m^2} T^{5/2}. \quad (28)$$

The energy relaxation rates are expressed via the corresponding rates $1/\tau_m$ that are given by Eqs. (27) and (28) by the relationship of Eq. (26), where the factor $9\zeta(9/2)/\zeta(7/2)$ is replaced by $7\zeta(7/2)/\zeta(5/2)$. Thus in a film with stress-free surfaces, which make contact with metal, the relaxation of a 2DEG is more effective than the relaxation in a film in contact with vacuum.

Note that the influence of the surface metallization on the PA scattering is different for a 2D electron channel placed in thin films and near a surface of semi-infinite media.²⁹ For the latter screening is suppressed, similar to the case of a thin film, providing an enhancement of the electron-acoustic phonon interaction. However, the unscreened matrix element in the vicinity of the metal is suppressed in such a way that—in the final result—metallization does not change the temperature dependence of the relaxation rates. But in the case of the film, the overall influence of metal results in the enhancement of the PA electron-phonon interaction.

For DP scattering, the factor of the high density of states occurs to be so strong that it leads to relaxation rate enhancement despite the almost transverse character of the flexural modes. As we see from Eq. (20), the value of V_{DP} for flexural modes at small q is less than that for the almost longitudinal dilatational modes. For PA scattering, the enhancement of the electron relaxation occurs to a lesser degree. Qualitatively, this is because of the nonlocal character of the PA interaction. Acoustic vibrations in the film induce an electric field not only inside the film, but also in the regions surrounding the film. The electric field outside the film decays exponentially with the characteristic length determined by the inverse phonon wave vector. At low temperatures $T \ll T_f$, the major contribution to the relaxation rates is provided by phonons with a value of $1/q$ much larger than the film thickness. This means that the electric field “spreads” over large distances; its value inside the film decreases, and the PA interaction of electrons with phonons becomes less effective. Similar arguments are also valid for the case of a metallized film. Although the electric field in this case is zero outside the film, its value inside the film is reduced as a result of screening by the electrons of the metal.

It is important to mention that the reduction of the phonon dimensionality in itself leads to an increase in the phonon density of states. As a result, for the DP interaction, the contribution of dilatational modes having a linear dispersion exceeds the relaxation rates for the case of bulk phonons. For the PA interaction, however, the effect of the electric field “spread” prevails over the effect caused by the phonon den-

sity of states for dilatational and horizontal shear modes, and their contributions to the relaxation rates are less than the values for the scattering on bulk phonons.

An important peculiarity of the obtained results is that DP and PA interactions cause the same temperature dependence of the relaxation rates. For the case of interaction with bulk phonons, the PA scattering is stronger than the DP scattering at temperatures lower than some critical value. The latter depends on the material parameters E_1 , e_{14} , and ϵ_f . Conversely, for the film, the relation between the strengths of the DP and PA scatterings does not depend on the temperature. The ratio between the relaxation rates due to DP and PA scatterings is

$$\frac{\tau^{(PA)}}{\tau^{(DP)}} \sim \left(\frac{E_1 \epsilon_f \epsilon_0}{e e_{14} a} \right)^2. \quad (29)$$

As we see, besides the material parameters, this ratio depends on the film thickness. For GaAs parameters³⁴ and $a = 10$ nm we obtain that the ratio of Eq. (29) is of the order of 0.3. As we see, for such parameters the DP and PA contributions to the relaxation rates are of the same order.

It is also important to stress that the potential energy of DP interaction for flexural modes, $V_{DP}^{(f)}$, is an odd function of z . As a result, if the electron wave function $\chi(z)$ is even, the matrix element of the DP electron-phonon interaction for flexural modes vanishes, and the asymptotic formulas for the relaxation rates should be rewritten in order to incorporate the scattering on the dilatational modes. Finally, in this case the enhancement of the relaxation rates with respect to the bulk phonons is less pronounced. Such symmetry holds, for example, for the free-standing quantum wells (QWs). However, even for them the interaction with the flexural modes can be switched on by the electric field applied perpendicular to the film surface, which breaks the symmetry of $\chi(z)$.

Let us now consider the case of a film with rigid surfaces. The main peculiarity of the phonon spectrum in such films is the existence of a forbidden gap of the width $\Delta\omega \sim \pi s_t/a$ at $q \rightarrow 0$. This restricts electron scattering at low temperatures: $T < \hbar\Delta\omega \sim T_f$. From Eq. (18) it was found that for $T \ll T_f$ the relaxation rates are exponentially small:

$$\frac{1}{\tau_{m,e}} \sim \exp\left(-\frac{\hbar\Delta\omega}{T}\right). \quad (30)$$

This result is common for the DP and PA mechanisms of the electron-phonon interaction.

V. RESULTS OF THE NUMERICAL CALCULATIONS AND DISCUSSION

To trace the temperature dependence of the relaxation rates more rigorously and to find those at intermediate temperatures, we carried out numerical calculations. These calculations take into account interaction with all phonon branches and exact expressions for the potentials V_{DP} and $\tilde{\phi}_{PA}$, as well as the phonon spectrum obtained by means of the numerical solution of the dispersion equations. The calculations were carried out for GaAs material parameters³⁴

and a 5-nm QW with infinite barriers whose center is situated at a distance 2 nm from the midplane of the 10-nm film. The electron concentration was 10^{11} cm^{-2} . The model of infinite barriers is good enough for many actual heterostructures. For example, for GaAs/AlAs heterostructures the barrier for electrons is about 1 eV, which is great enough to treat it as infinite for a 5-nm QW where the energy of ground level is about 100 meV.

In Figs. 3 and 4 the temperature dependencies of the relaxation rates for the DP and PA mechanisms for films with stress-free surfaces are shown. The results for films with rigid surfaces are presented in Figs. 5 and 6. Three types of electrical boundary conditions were studied: the case when the film is surrounded by vacuum ($\epsilon_s = 1$), a medium with the same dielectric constant $\epsilon_s = \epsilon_f$, and a metal $\epsilon_s = \infty$. For comparison, the corresponding temperature dependence of the relaxation rates due to scattering on bulk phonons is shown on each plot. As we see, for a film with free surfaces—Figs. 3 and 4—the behavior of the DP and PA relaxation rates is qualitatively different if we compare them with the bulk-phonon values. For the DP interaction, the temperature dependence is quite close to the asymptotic expressions of Eqs. (21) and (26). That is, for sub-Kelvin temperatures the relaxation rates are enhanced strongly with respect to those for interaction with bulk phonons, exceeding the latter by *several orders of magnitude*. Conversely, for the PA interaction the behavior of the relaxation rates is more complex, especially for the case of energy relaxation. This is mainly because for PA scattering the enhancement of the contribution of the flexural phonon modes is less pronounced than for DP scattering, while the contributions of the dilatational and horizontal shear modes is less than the bulk value. As a result, depending on the temperature, the relaxation rates can be larger or smaller than for the bulk. In particular, for some temperatures the PA relaxation rates can be of the order of magnitude *lower* than the bulk value, and the asymptotic dependencies obtained in Sec. IV can be observed only for very low temperatures, where the criterion $T \ll T_f$ is well fulfilled. Respectively, such a complex behavior leads to a relatively weak difference between the relaxation rates in the film and in the bulk when we consider simultaneous action of the DP and PA mechanisms. According to these results, the strong enhancement of the electron relaxation in thin free-surface films is likely to occur in non-piezoelectric materials, where only DP scattering is present, such as Si, Ge, etc. For multivalley semiconductors, another qualitative feature is important. That is, electrons in them can interact with transverse phonons via the DP mechanism. In bulk materials this peculiarity does not change the temperature dependence of the relaxation rates, since both longitudinal and transverse phonons have linear dispersions. For films, however, the situation is different. As we see from Eq. (20), the DP potential energy for flexural modes is proportional to q^2 . This is because long-wavelength flexural modes are almost transverse, and the DP interaction is partially suppressed for Γ -valley electrons. Conversely, for multivalley semiconductors the transverse character of flexural modes does not suppress DP scattering, in general, and one can expect an even stronger enhancement of DP relaxation rates

with respect to the bulk characteristics.

Even more pronounced results are obtained for the electron relaxation in a rigid-surface film. Here the relaxation rates are suppressed exponentially in accordance with Eq. (30). Note, however, that this result should be applied for real structures very cautiously. This is because the model of a rigid-surface film is somewhat artificial. As opposed to a suspended film which is completely isolated, the rigid-surface condition can be obtained for a film sandwiched between the layers of a very rigid material. Rigorously, in such a system there are two kinds of phonon modes. First, there are phonons confined in the film. For such phonons, the gap in the spectrum really exists. Apart from these, there are phonons penetrating to the film from the surrounding layers. They have a 3D-like spectrum without a gap. However, such phonons have a relatively small density of states due to the large value of the sound velocity in the surrounding material, and we expect that their interaction with electrons in the film is relatively weak. Note that similar behavior holds for a film with one rigid surfaces and one free surface. We have obtained a phonon dispersion equation and found that a low-frequency gap exists for such a system as well. To analyze the abovementioned system quantitatively, it is necessary to find the phonon spectrum using the general boundary conditions at the film surface in contact with a semi-infinite medium, which will be done in a subsequent publication. It should also be mentioned that a fabrication of the rigid-surface films is not an easy technological problem. This is because it is quite difficult to find materials having considerable elastic mismatch and, simultaneously, a good-quality interface. Perhaps, such structures can be fabricated using the epitaxial lift-off method,³⁵ allowing a fusing of a film with thickness of about several tenths of a micron to a substrate. Originally, this method was used for the deposition of the GaAs film on a LiNbO₃ crystal, whose sound velocity is considerably higher than that of GaAs. A stronger elastic mismatch could be obtained in the case of deposition on a diamond or sapphire substrates. For such relatively thick films, however, the phonon confinement should be manifested at lower temperatures, less than 100 mK.

The calculation method derived in the present paper allows one to investigate the electron relaxation process in the less sophisticated system than a 2DEG inside a film: a metal or semiconductor film with 3D electrons, where the role of the acoustic phonon confinement should be very important as well. Such a study is important, for example, for the control of energy relaxation in modern detector structures.³⁶ Note that previously some authors detected an anomalous temperature dependence of the electron scattering rates in thin metal films at low temperatures.^{37,38} Although the role of the reduction of the phonon dimensionality was proposed as a possible reason for the modification of the electron-phonon interaction in Ref. 38, the role of specific phonon properties in films (for example, the appearance of flexural phonons in the suspended films) was not discussed.

Note that the energy relaxation rate of hot electrons is directly determined by the electron-phonon interaction, while the phonon contribution to the electron mobility should be separated on the background of other scattering mechanisms

employing Matheissen's rule. Experiments with hot electrons^{39,21} as well as mobility measurements⁴⁰ were successfully used to study peculiarities of the electron-phonon interaction in semiconducting structures with bulk phonon spectrum. In particular, the techniques used in Refs. 39 and 21 allows energy relaxation measurements for weak levels of excitation, that assures a probing of the phonon confinements. The problem of close-to-equilibrium measurements can be more important in the case of free-standing films. This is because in such films the removal of the phonons occurs only through the edges of the film; as a result, a considerable buildup of the nonequilibrium phonons can be manifested even at weak electric fields. This would give rise to phonon drag and a phonon bottleneck in the electron energy relaxation. We analyze these issues in Appendix C. According to this analysis, the phonon buildup should not be manifested in films whose length is much less than some critical value; for a GaAs film with a thickness of about 10 nm, this critical length is about 1 mm. In addition, even in long films the phonon buildup is unimportant in the case of transient measurements. This especially concerns the energy relaxation process, which is a direct result of the low heat capacity of degenerate electrons. We believe that our results will stimulate experiments with nanostructures, where phonon confinement significantly modifies the electron energy relaxation rate and phonon contribution to the mobility.

VI. CONCLUSIONS

In conclusion, we have analyzed in detail the peculiarities of 2D electron interactions via the deformation potential and piezoelectric mechanisms with completely confined acoustic phonons in thin films. It is shown that, at low temperatures, when the electrons can interact only with a few phonon modes, the peculiarities of the phonon spectrum drastically modify the temperature dependence of the electron momentum and energy relaxation rates. In particular, the relaxation rates are found to be very sensitive to the mechanical and electrical conditions at the surface. For films with stress-free surfaces, the relaxation rates normally become larger than for the interaction with bulk phonons, especially for the deformation potential mechanism of interaction. This is a direct result of the high density of states of the confined phonons. It was found that at low temperatures, the momentum and energy relaxation rates for such a film are proportional to $T^{7/2}$ for both DP and PA interactions, which is essentially different from the scattering of 2DEG in the bulk materials. Moreover, for metallized films, the enhancement of the relaxation rates becomes even more pronounced due to the suppression of screening, leading to a $T^{5/2}$ dependence of the relaxation rates. Conversely, if the surface of the film is rigid, the relaxation rates at low temperatures become exponentially small due to formation of a gap in the phonon spectrum. These results demonstrate a way of electron-phonon relaxation tailoring by means of phonon control in the modern heterostructures.

ACKNOWLEDGMENTS

This work was supported by the U.S. Army Research Office.

APPENDIX A: ACOUSTIC PHONON MODES IN FREE-STANDING AND RIGID-SURFACE FILMS

Here we summarize the obtained results for the spectrum and eigen displacements of the acoustic phonons in free-standing and rigid-surface films. Let us begin with the case of free-standing films. For the dilatational modes the dispersion equation is

$$\tan \frac{k_t a}{2} + \frac{4q^2 k_l k_t}{(q^2 - k_t^2)^2} \tan \frac{k_l a}{2} = 0, \quad (\text{A1})$$

where

$$k_l = \sqrt{\frac{\omega^2}{s_l^2} - q^2}, \quad k_t = \sqrt{\frac{\omega^2}{s_t^2} - q^2}. \quad (\text{A2})$$

The eigendisplacements can be written as

$$u_{0d}^{(\parallel)} = iA_d q \left((q^2 - k_t^2) \sin \frac{k_l a}{2} \cos k_l z + 2k_l k_t \sin \frac{k_l a}{2} \cos k_l z \right),$$

$$u_{0d}^{(z)} = -A_d k_l \left((q^2 - k_t^2) \sin \frac{k_l a}{2} \sin k_l z - 2q^2 \sin \frac{k_l a}{2} \sin k_l z \right), \quad (\text{A3})$$

where A_d is the arbitrary constant.

For flexural modes the dispersion equation and displacements are

$$\tan \frac{k_l a}{2} + \frac{4q^2 k_l k_t}{(q^2 - k_t^2)^2} \tan \frac{k_t a}{2} = 0, \quad (\text{A4})$$

$$u_{0f}^{(\parallel)} = iA_f q \left((q^2 - k_t^2) \cos \frac{k_l a}{2} \sin k_l z + 2k_l k_t \cos \frac{k_l a}{2} \sin k_l z \right),$$

$$u_{0f}^{(z)} = A_f k_l \left((q^2 - k_t^2) \cos \frac{k_l a}{2} \cos k_l z - 2q^2 \cos \frac{k_l a}{2} \cos k_l z \right). \quad (\text{A5})$$

The displacement associated with the shear modes is given by

$$u_{0s}^{(\perp)}(z) = A_s \begin{cases} \cos k_{tj} z, & \text{if } j=0,2,\dots \\ \sin k_{tj} z, & \text{if } j=1,3,\dots, \end{cases} \quad (\text{A6})$$

where $k_{tj} = \pi j/a$. The dispersion relation for shear waves is $\omega_j = s_t \sqrt{k_{tj}^2 + q^2}$.

Let us proceed with the case of rigid-surface films. The dispersion equation and the eigendisplacements are given by

$$\tan \frac{k_l a}{2} + \frac{q^2}{k_l k_t} \tan \frac{k_t a}{2} = 0, \quad (\text{A7})$$

$$u_{0d}^{(\parallel)} = iA_d q \left(\cos \frac{k_l a}{2} \cos k_l z - \cos \frac{k_t a}{2} \cos k_l z \right),$$

$$u_{0d}^{(z)} = -A_d k_l \cot \frac{k_t a}{2} \left(\sin \frac{k_l a}{2} \sin k_l z - \sin \frac{k_t a}{2} \sin k_l z \right) \quad (\text{A8})$$

for the dilatational modes, and by

$$\tan \frac{k_t a}{2} + \frac{q^2}{k_l k_t} \tan \frac{k_l a}{2} = 0, \quad (\text{A9})$$

$$u_{0f}^{(\parallel)} = iA_f q \left(\sin \frac{k_l a}{2} \sin k_l z - \sin \frac{k_t a}{2} \sin k_l z \right),$$

$$u_{0f}^{(z)} = A_f k_l \tan \frac{k_t a}{2} \left(\cos \frac{k_l a}{2} \cos k_l z - \cos \frac{k_t a}{2} \cos k_l z \right) \quad (\text{A10})$$

for the flexural modes.

The displacements of shear modes are given by

$$u_{0s}^{(\perp)}(z) = A_s \begin{cases} \cos k_{tj} z & \text{if } j=1,3,\dots \\ \sin k_{tj} z, & \text{if } j=2,4,\dots, \end{cases} \quad (\text{A11})$$

where k_{tj} are the same as for the shear modes in free-standing films.

We label the solutions of Eq. (1), i.e., eigenvectors $\mathbf{u}(\mathbf{r}, z, t)$, by the complex quantum number $\lambda = (\nu, j, q)$, where $\nu = d, f, s$ stand for the types of modes, and j labels the branches $\omega_j(q)$. The set of complex-valued vectors $\mathbf{u}_\lambda(\mathbf{r}, z) = \mathbf{u}_{0\lambda}(z) \exp(i\mathbf{q}\mathbf{r})$ represents a full system of orthogonal functions in a volume $V = aS$. The constants $A_\nu(\omega_j, q)$ are determined by the normalization rule

$$\int_{(V)} d\mathbf{r} dz [\mathbf{u}_\lambda(\mathbf{r}, z) \cdot \mathbf{u}_\lambda^*(\mathbf{r}, z)] = 1. \quad (\text{A12})$$

This provides the condition that each mode carries energy $\hbar\omega$ in volume V , that is necessary for the procedure of quantization of the acoustic waves. In the so-called ‘‘second quantization representation,’’ the phonon displacement operator takes the form

$$\hat{\mathbf{u}} = \sum_\lambda \left(\frac{\hbar}{2\rho\omega_\lambda S} \right)^{1/2} [\mathbf{u}_{0\lambda}(z) e^{i(\mathbf{q}\mathbf{r} - \omega_\lambda t)} \hat{b}_\lambda + \text{H.c.}], \quad (\text{A13})$$

where \hat{b}_λ is a phonon annihilation operator, ρ represents the density.

APPENDIX B: SCREENING FACTOR OF 2D ELECTRONS CONFINED INSIDE A FILM

To determine screening of the electron-phonon interaction potential energy V_{e-ph} , one should take into account the potential energy V_{el} induced by the perturbation of the electron density δn in the resulting field, $V = V_{e-ph} + V_{el}$. For V_{el} we have the Poisson equation

$$\frac{d^2 V_{el}}{dz^2} - q^2 V_{el} = -\frac{e^2}{\epsilon_f \epsilon_0} \delta n. \quad (\text{B1})$$

The redistribution of δn is determined by the total perturbation V . On the boundaries of discontinuity, $z = \pm a/2$, standard boundary conditions for the potential are applied. For the matrix element of the resulting perturbation V , one obtains

$$\int V\chi^2(z)dz = \frac{1}{\epsilon} \int V_{e-ph}\chi^2(z)dz, \quad (\text{B2})$$

where ϵ is a dynamical screening factor:

$$\epsilon(\omega, q) = 1 + \frac{e^2}{2q\epsilon_f\epsilon_0} \Pi(\omega, q)(\Phi_1 + \Phi_2). \quad (\text{B3})$$

Here $\Pi(\omega, q)$ is the random phase approximation polarization function.⁴¹ The zero-temperature expression for $\Pi(\omega, q)$ is given by a simple analytic expression;⁴¹ for nonzero temperatures $\Pi(\omega, q, T)$ has been expressed in terms of $\Pi(\omega, q, T=0)$ in Ref. 42, and calculated in detail in Ref. 43. The functions Φ_1 and Φ_2 are defined by the equations

$$\begin{aligned} \Phi_1 &= \int \chi^2(z)dz \int \chi^2(z')\exp(-q|z-z'|)dz', \\ \Phi_2 &= \frac{2\chi_+\chi_-\exp(-qa)(\epsilon_s - \epsilon_f)^2 - (\chi_-^2 + \chi_+^2)(\epsilon_s^2 - \epsilon_f^2)}{\exp(qa)(\epsilon_s + \epsilon_f)^2 - \exp(-qa)(\epsilon_s - \epsilon_f)^2}, \end{aligned} \quad (\text{B4})$$

where $\chi_{\pm} = \int dz \exp(\pm qz)\chi^2(z)$, and ϵ_f and ϵ_s are the dielectric constants of the film and surrounding material, respectively.

Note that the form factors χ_{\pm} and hence $\epsilon(\omega, q)$ depend on the quantum-well (QW) position. In the simplest case, when electrons are degenerate, $\hbar\omega \ll \epsilon_F$ and $q \ll k_F$, the function $\Pi(\omega, q)$ is reduced to the constant $\Pi \approx m/\pi\hbar^2$, and Eq. (B3) can be rewritten as

$$\epsilon = 1 + \frac{2}{a_B q} (\Phi_1 + \Phi_2), \quad (\text{B5})$$

where $a_B = 4\pi\epsilon_0\epsilon_f\hbar^2/e^2m$ is the effective Bohr radius. Going further, for $qa_B \ll 1$, $qa \ll 1$ we have

$$\epsilon = \frac{2}{a_B q} \frac{\epsilon_f}{\epsilon_s}, \quad (\text{B6})$$

where ϵ_s was assumed to be finite. The analogous screening factor of 2D electrons placed in the bulk is $\epsilon_{bulk} = 2/(a_B q)$, i.e., in films, screening of long-wavelength phonons is enhanced for $\epsilon_s < \epsilon_f$ and suppressed for $\epsilon_s > \epsilon_f$. The limiting case of metallized films can be obtained by putting $\epsilon_s = \infty$ in Eq. (B4). For a 2DEG confined in a rectangular infinitely deep QW with width d we obtain

$$\epsilon_m = 1 + \frac{a}{a_B} \left[1 - 4\frac{z_0^2}{a^2} - \frac{2d}{3a} \left(1 - \frac{15}{4\pi^2} \right) \right] \quad (\text{B7})$$

in the limit of small q . Here z_0 is the distance from a center of the film to a center of a QW. One can see that for a metallized film in the long-wavelength limit the screening factor is of the order of unity and does not depend on q .

APPENDIX C: ESTIMATE OF THE NONEQUILIBRIUM PHONON BUILDUP IN FREE-STANDING FILMS

In free-standing films, the relaxation of the phonons emitted by electrons to equilibrium is a slow process at low temperatures. This is because, first, the scattering of phonons due to the lattice anharmonicity and defects is characterized by small rates, and, second, because ballistic removal of phonons occurs only through the edges of finite-length films. Obviously, if the length of the film, L , is large enough, this should cause a considerable buildup of the nonequilibrium phonons even at low electric field and, consequently, a decrease of both momentum and energy relaxation rates. Here we are going to estimate the critical length L_c , at which the buildup of the nonequilibrium phonons becomes important. We consider the momentum relaxation first, assuming that electric field and, consequently, the electron drift velocity and deviation of the phonon population from equilibrium are small. The electron momentum balance equation, taking into account the nonequilibrium character of the phonon distribution, is

$$m\frac{dv_{dr}}{dt} = eF - \frac{mv_{dr}}{\tau_m} + \mathcal{F}\{\delta N_{\lambda}\}, \quad (\text{C1})$$

where the term \mathcal{F} describes drag due to the nonequilibrium phonons. The phonon distribution function can be written down as $N_{\lambda} = N_{\omega} + \delta N_{\lambda}$, where N_{ω} is the Planck function and, as in Appendix A, λ labels the phonon modes. For N_{λ} the following kinetic equation can be introduced:

$$\frac{dN_{\lambda}}{dt} = P_{\lambda}^{(em)}(1 + N_{\lambda}) - P_{\lambda}^{(ab)}N_{\lambda} - \beta(N_{\lambda} - N_{\omega}). \quad (\text{C2})$$

Here $P_{\lambda}^{(em,ab)}$ are the rates of the phonon emission and absorption, and β is the phenomenological parameter characterizing removal of the nonequilibrium phonons. Equation (C2) can be rewritten as

$$\frac{d\delta N_{\lambda}}{dt} = G - (\alpha + \beta)\delta N_{\lambda}, \quad (\text{C3})$$

where G describes the process of the nonequilibrium phonon generation by the electron drift (G is proportional to v_{dr}) and $\alpha = P_{0\lambda}^{(ab)} - P_{0\lambda}^{(em)}$, $P_{0\lambda}^{(em,ab)}$ being the rates of the phonon emission and absorption with $v_{dr} = 0$. Here we do not provide explicit expressions for \mathcal{F} , G , and α , which can be obtained in a straightforward manner with the use of the previously derived Hamiltonian of the electron-phonon interaction.

From Eq. (C3), in the steady state, $\delta N_{\lambda} = G/(\alpha + \beta)$. It can be shown by direct calculations that if $\beta = 0$, then the last two terms in Eq. (C1) are mutually compensated and no steady state exists. Physically, this result is obvious: without the phonon removal, the electron-phonon system possesses no actual momentum relaxation. Therefore, if for a typical phonon $\beta \gg \alpha$, then $\mathcal{F} \ll mv_{dr}/\tau_m$ and the phonon drag does not modify essentially the electron transport. An analogous

consideration of the electron energy balance provides a similar criterion for the role of the nonequilibrium phonons in the electron energy relaxation.

Using the previously derived Hamiltonian of the electron-phonon interaction, results for the phonon spectrum, and the screening factor, α can be easily calculated. For flexural phonons with $\hbar\omega \approx T$, $T < T_f$, and DP coupling, we obtain the following approximate expression:

$$\alpha \approx \frac{E_1^2 T^{5/2} m^{3/2} a_B^2}{a^{3/2} s^{5/2} \hbar^{9/2} \rho \epsilon_F^{1/2}} \left(\frac{\epsilon_s}{\epsilon_f} \right)^2. \quad (\text{C4})$$

Here we assumed that the quantum well and film widths are of the same order. Since we aim to make a rough estimate we do not take into account the difference between the longitudinal and transverse sound velocities, and just put some ‘‘average’’ sound velocity s in Eq. (C4). Provided that the phonon-phonon scattering and phonon scattering by defects is weak, only a ballistic removal of the phonons from the film is important. In this case, which corresponds to the lower limit of β , we can estimate $\beta \approx g/L$, where g is the group velocity of thermal phonons. Finally, for L_c we have an approximate expression

$$L_c = \frac{a^2 s^3 \rho \hbar^4 \epsilon_F^{1/2}}{E_1^2 T^2 a_B^2 m^{3/2}} \left(\frac{\epsilon_f}{\epsilon_s} \right)^2. \quad (\text{C5})$$

For the system parameters used in our calculations, $\epsilon_s = \epsilon_f$, and $T = 1$ K, we obtain $L_c \sim 1$ mm. Therefore, the buildup of the nonequilibrium phonons should not be manifested in films of length about tens of microns or less. Direct calculations for dilatational and shear phonons show that, for them, buildup occurs in even longer films; this is because of the stronger screening of the thermal phonon coupling with electrons. For piezoelectric scattering, E_1 in Eq. (C5) should be substituted for by $ee_{14a}/(\epsilon_0 \epsilon_f)$. For $a \sim 10$ nm, these values are of the same order of magnitude and, therefore, provide similar L_c .

On the other hand, the film should be long enough to ensure the diffusive electron transfer. Thus L must satisfy the condition $L > L_e = v_F \tau_{ee}$, where v_F is the electron Fermi velocity and τ_{ee} is the characteristic time of electron-electron scattering. Using the estimate for the τ_{ee} mentioned in Sec. III, we can obtain

$$\frac{L_c}{L_e} \approx \frac{a^2 s^3 \rho \hbar^3}{E_1^2 a_B^2 m \epsilon_F} \left(\frac{\epsilon_f}{\epsilon_s} \right)^2. \quad (\text{C6})$$

This ratio is about 100, which is high enough to provide simultaneously diffusive electron transfer and fast removal of the phonons in films with $L_e < L < L_c$. Note that the simple expression we used for the electron-electron scattering time overestimates τ_{ee} (see Ref. 44), and that the ratio of Eq. (C6) can be even higher, which facilitates the achievement of this condition.

So far, we treated only the steady-state case. However, it is possible to show that a buildup of the nonequilibrium phonons should not be manifested in transient measurements even in long films. Indeed, according to Eq. (C1), in the absence of nonequilibrium phonons the steady-state drift velocity is onset with a characteristic time on the order of τ_m . On the other hand, the steady-state phonon distribution is onset with a characteristic time of about $1/\alpha$. Using the expressions for $1/\tau_m$ [Eq. (21)], and α , we can write

$$\frac{1}{\tau_m} \approx \alpha \frac{T}{\epsilon_F} \left(\frac{\hbar}{sam} \right)^2. \quad (\text{C7})$$

Since $\hbar/(sam) \approx 100$ for $a = 10$ nm, at not too low temperatures the quasi-steady-state drift velocity is onset before a substantial buildup of the nonequilibrium phonons. Let us now turn to the energy relaxation. The energy balance equation is

$$\frac{dE}{dt} = Wn - n \frac{T_e - T}{\tau_e}, \quad (\text{C8})$$

where E is the average electron energy per unit area and W is the power input to the electron subsystem per unit area. Therefore, the onset of the electron temperature occurs on the time scale $\tau_T = \tau_e c_e / n$, where c_e is the electron heat capacity. For degenerate 2D electrons, $c_e = \pi m T / (3 \hbar^2)$. So, using the results for τ_e , [Eqs. (21) and (26)], we obtain

$$\frac{1}{\tau_T} \approx \alpha \frac{\hbar}{sam}. \quad (\text{C9})$$

This means that for typical film the quasi-steady-state electron temperature onsets before the phonon buildup takes place. In contrast to the case of the drift velocity onset, this occurs at an arbitrarily low temperature.

¹P.J. Price, J. Appl. Phys. **53**, 6863 (1982).

²B.K. Ridley, *Electrons and Phonons in Semiconductor Multilayers* (Cambridge University Press, Cambridge, 1997).

³*Phonons in Semiconductor Nanostructures*, Vol. 236 of NATO Advanced Study Institute, Series E: Applied Sciences, edited by J.-P. Leburton, J. Pascual, and C.S. Torres (Kluwer, Dordrecht, 1993).

⁴M. Dutta, M.A. Stroschio, and K. W. Kim, in *Quantum-Based Electronic Devices and Systems*, edited by M. Dutta and M.A. Stroschio (World Scientific, Singapore, 1998).

⁵N. Bannov, V. Aristov, V. Mitin, and M. Stroschio, Phys. Rev. B **51**, 9930 (1995).

⁶M. Grimsditch, R. Bhadra, and I. Schuller, Phys. Rev. Lett. **58**, 1216 (1987).

⁷J.C. Nability and M.N. Wybourne, Phys. Rev. B **42**, 9714 (1990); **44**, 8990 (1991).

⁸T.S. Tighe, J.M. Worlock, and M.L. Roukes, Appl. Phys. Lett. **70**, 2687 (1997); K. Schwab, E.A. Henriksen, J.M. Worlock, and M.L. Roukes, Nature (London) **404**, 974 (2000).

⁹S.M. Komirenko, K.W. Kim, M.A. Stroschio, and V.A. Kochelap, Phys. Rev. B **58**, 16360 (1998).

¹⁰M.A. Stroschio and K.W. Kim, Phys. Rev. B **48**, 1936 (1993).

¹¹S. Yu, K.W. Kim, M.A. Stroschio, G.J. Iafrate, and A. Ballato, Phys. Rev. B **50**, 1733 (1994).

- ¹²S. Yu, K.W. Kim, M.A. Stroscio, and G.J. Iafrate, Phys. Rev. B **51**, 4695 (1995).
- ¹³T.D. Krauss and F.W. Wise, Phys. Rev. Lett. **79**, 5102 (1997).
- ¹⁴M.A. Stroscio and M. Dutta, Phys. Rev. B **60**, 7722 (1999).
- ¹⁵K. Schwab, W. Fon, E. Henriksen, J.M. Worlock, and M.L. Roukes, Physica B **280**, 458 (2000).
- ¹⁶M.P. Blencowe, Phys. Rev. B **59**, 4992 (1999).
- ¹⁷M.L. Roukes, Physica B **263-264**, 1 (1999).
- ¹⁸R. Lifshitz and M.L. Roukes, Phys. Rev. B **61**, 5600 (2000).
- ¹⁹B.A. Glavin, Phys. Rev. Lett. **86**, 4318 (2001).
- ²⁰D.J. Thouless, Phys. Rev. Lett. **39**, 1167 (1977).
- ²¹S.-H. Song, W. Pah, D.C. Tsui, Y.H. Xie, and D. Monroe, Appl. Phys. Lett. **70**, 3422 (1997).
- ²²K. Misawa, H. Yao, T. Hayashi, and T. Kobayashi, J. Chem. Phys. **94**, 4131 (1991).
- ²³H.-S. Yang, K.S. Hong, S.P. Feofilov, B.M. Tissue, R.S. Meltzer, and W.M. Dennis, J. Lumin. **83-84**, 139 (1999).
- ²⁴N. Bannov, V. Aristov, and V. Mitin, Solid State Commun. **93**, 483 (1995); J. Appl. Phys. **78**, 5503 (1995).
- ²⁵V.I. Pipa, B.A. Glavin, V.V. Mitin, and M.A. Stroscio, Semicond. Sci. Technol. **13**, A97 (1998).
- ²⁶N. Bannov, V.V. Mitin, and M. Stroscio, Phys. Status Solidi B **183**, 131 (1994).
- ²⁷C. Hodges, H. Smith, and J.W. Wilkins, Phys. Rev. B **4**, 302 (1971).
- ²⁸A. Knäbchen, Y.B. Levinson, and O. Entin-Wohlman, Phys. Rev. B **54**, 10 696 (1996).
- ²⁹V.I. Pipa, N.Z. Vagidov, V.V. Mitin, and M. Stroscio, Physica B **270**, 280 (1999).
- ³⁰*Handbook of Mathematical Functions*, edited by M. Abramowitz and I. Stegun (National Bureau of Standards, Washington, DC, 1964).
- ³¹P.J. Price, Solid State Commun. **51**, 607 (1984); Surf. Sci. **143**, 145 (1984).
- ³²T.J. Gramila, J.P. Eisenstein, A.H. MacDonald, L.N. Pfeiffer, and K.W. West, Phys. Rev. Lett. **66**, 1216 (1991); Phys. Rev. B **47**, 12 957 (1993).
- ³³L. Swerkovski, J. Szymanski, and Z.W. Gortel, J. Phys.: Condens. Matter **8**, L295 (1996).
- ³⁴We use the material parameters $E_1=8$ eV, $e_{14}=0.16$ C/m², $\epsilon_f=12.5$, $s_l=5.2\times 10^5$ cm/s, $s_t=3.02\times 10^5$ cm/s, $\rho=5.2$ g/cm³, and $m=0.067m_0$, which are close to the GaAs parameters.
- ³⁵E. Yablonovitch, D.M. Hwang, T.J. Gmitter, L.T. Florez, and J.P. Harbison, Appl. Phys. Lett. **56**, 2419 (1990).
- ³⁶A.V. Sergeev and M.Yu. Reizer, Int. J. Mod. Phys. B **10**, 635 (1996).
- ³⁷J. Liu and N. Giordano, Phys. Rev. B **43**, 3928 (1991).
- ³⁸J.F. DiTusa, K. Lin, M. Park, M.S. Isaacson, and J.M. Parpia, Phys. Rev. Lett. **68**, 1156 (1992).
- ³⁹A.A. Verevkin, N.G. Ptitsina, G.M. Chulcova, G.N. Gol'tsman, E.M. Gershenzon, and K.S. Yngvesson, Phys. Rev. B **53**, R7592 (1996).
- ⁴⁰H.L. Stormer, L.N. Pfeiffer, K.W. Baldwin, and K.W. West, Phys. Rev. B **41**, 1278 (1990).
- ⁴¹F. Stern, Phys. Rev. Lett. **18**, 546 (1967).
- ⁴²P.F. Maldague, Surf. Sci. **73**, 296 (1978).
- ⁴³K. Flensberg and B.Y. Hu, Phys. Rev. B **52**, 14 796 (1995).
- ⁴⁴S.-C. Lee and I. Galbraith, Phys. Rev. B **59**, 15 796 (1999).